with the observation of a Newtonian flow at very low frequencies. It would be interesting to perform a similar analysis on sulfonated EPDM's with ionic interacting groups. On the other hand, for SBS-type thermoplastic elastomers an equilibrium modulus has been calculated by using a similar type of analysis. This substantiates the conclusion that thermoreversible network structures formed by randomly distributed functional groups are of a different nature than phase-separated systems.

The general effect on interacting groups is a shift of the terminal relaxation times to long times by imposing additional restrictions on the relaxing chains. By the same restrictions, the plateau modulus is increased. In many applications, where deformation is only applied for short times, or good damping properties are required over an expanded time scale, such thermoreversible associations may be sufficient.

The present study clearly reveals the relation between molecular parameters, such as primary molecular weight and degree of modification, and viscoelastic properties of polymer melts with strongly interacting functional groups. Nevertheless several problems remain to be solved for these systems. A quantitative analysis requires the knowledge of the fraction of hydrogen bonds formed. A preliminary study shows that the fraction of free and bound units may be derived from IR spectroscopy.[11] These studies are presently extended to a wider range of temperatures and for different degrees of modification. In this context it is important to determine whether the thermodynamic equilibrium concentration of hydrogen bonds of analogous low molecular weight model compounds is reached in polymer melts, or whether topological restrictions imposed on the interacting groups, because they are fixed to a polymer backbone, become important.

To study the structure of the thermoreversible aggregates different methods must be applied. The structures formed by thermoreversible association will be accessible from light-scattering measurements in the dilute and semidilute regime.

Acknowledgment. Financial support from Stiftung Volkswagenwerk through the Joint Project Freiburg-Porto Alegre is gratefully acknowledged. L.L.F. thanks the DAAD (German Academic Exchange Board) for her fellowship.

Registry No. I, 3232-84-6.

References and Notes

(1) Eisenberg, A.; Bailey, F. E., Eds. *Coulombic Interactions in Macromolecular Systems*; ACS Symposium Series; American Chemical Society: Washington, DC, 1986; Vol. 302.
(2) Hollday, L., Ed. *Developments in Ionic Polymers*; Applied Science: London, 1983.
(3) Joanny, J. F. *Polymer* **1980**, *21*, 71.
(4) Gonzales, A. E. *Polymer* **1983**, *24*, 77.
(5) Möller, M.; Omeis, J.; Muhleisen, E. In *Reversible Gelation in Polymers*; Russo, P., Ed.; ACS Symposium Series; American Chemical Society: Washington, DC, in press.
(6) Burchard, W. *Br. Polym. J.* **1985**, *17*, 154.
(7) Stadler, R.; Freitas, L. *Colloid Polym. Sci.* **1986**, *264*, 773.
(8) Leong, K. W.; Butler, G. B. *J. Macromol. Sci.* **1980**, *A-14*, 287.
(9) Butler, G. B. *Ind. Eng. Chem. Prod. Res. Dev.* **1980**, *19*, 512.
(10) Stadler, R.; Burgert, J. *Makromol. Chem.* **1986**, *187*, 1681.
(11) Stadler, R.; Freitas, L. *Polym. Bull.* **1986**, *15*, 173.
(12) Stadler, R.; Freitas, L., manuscript in preparation.
(13) Ferry, J. D. *Viscoelastic Properties of Polymers*, 3rd ed.; Wiley: New York, 1980.
(14) Tschoegl, N. W. *Rheol. Acta* **1971**, *10*, 582.
(15) Scholtens, B. J. R.; Booij, H. E. In *Elastomers and Rubber Elasticity*; Mark, J. E., Lal, J. Ed.; ACS Symposium Series; American Chemical Society: Washington, DC, 1982; Vol. 193, 157.
(16) Stadler, R.; Gronski, W. *J. Colloid Polym. Sci.* **1983**, *261*, 215.
(17) Stadler, R.; Freitas, L., unpublished results.
(18) Graessley, W. W.; Park, W. S.; Crawley, R. L. *Rheol. Acta* **1977**, *16*, 291.
(19) Raju, V. R.; Menezes, E. V.; Marin, G.; Graessley, W. W.; Fetters, L. J. *Macromolecules* **1981**, *14*, 1668.
(20) Carella, J. M.; Graessley, W. W.; Fetters, L. J. *Macromolecules* **1984**, *17*, 2775.
(21) Graessley, W. W. *Adv. Polym. Sci.* **1982**, *47*, 67.
(22) Cookson, R. C.; Gupte, S. S.; Stevens, J. D. R.; Watts, C. T. *Org. Synth.* **1971**, *51*, 121.
(23) Struglinski, M. J.; Graessley, W. W. *Macromolecules* **1985**, *18*, 2630.

Kinetic Observations by SAXS and Centrifugation of a Gelating System

Anne-Marie Hecht and Erik Geissler*

Laboratoire de Spectrométrie Physique,† Université Scientifique Technologique et Médicale de Grenoble, B.P. 87, 38402 St Martin d'Hères Cedex, France. *Received March 23, 1987*

ABSTRACT: We report observations from two distinct experiments of a system gelating in the presence of external constraints, an intense X-ray beam from a synchrotron source and the acceleration field of a centrifuge. In both these experiments on poly(acrylamide/bisacrylamide), a substantial fraction of the sample remains in the sol phase in coexistence with the developing gel. Kinetic observations by small-angle X-ray scattering (SAXS) and the Schlieren optics of the analytical centrifuge reveal that gelation is not necessarily the monotonic process that is found in samples gelling under uniform conditions, but can take the novel form of a series of separate gelation avalanches, each generation interpenetrating with the established structure of the previous gelation. These oscillations, fueled by monomers from the sol phase, are a consequence of the nonlinearities of the gelation process coupled with the delay due to diffusion of the monomers through the existing gel structure. The changes in the scattering function seen by SAXS permit comparisons with observations made by other authors on gelling systems.

Introduction

Gelating systems have recently been the object of much theoretical and experimental scrutiny, particularly with regard to which model best describes the sol–gel transition.[1] Close to this point, measurements of shear modulus,[2] viscoelasticity,[3] and permeability,[4] as well as light[5,6] and neutron[7] scattering measurements on interrupted polymerization reactions, have found broad agreement with the percolation model of gelation, the validity of which now seems generally accepted.

An important precaution taken in observations of ge-

† CNRS associate laboratory.

0024-9297/87/2220-2485$01.50/0

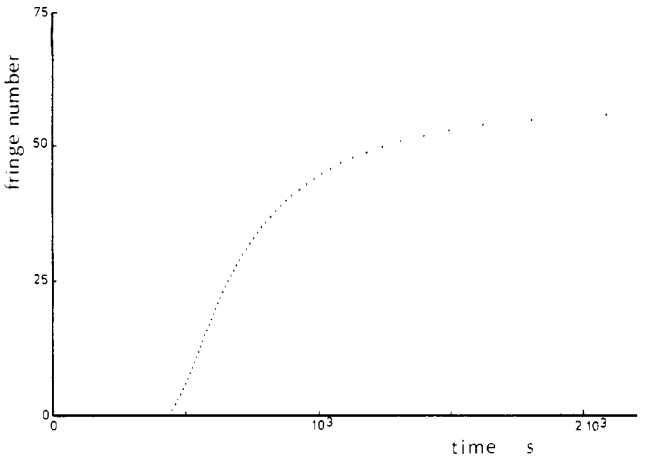

Figure 1. Observation of gelation in a uniform poly(acrylamide/bisacrylamide) sample (A = 0.06 g/mL, B = 0.002 g/mL) as a function of time after introduction of the accelerator (tetraethylenemethylenediamine). The sample, in a 1 × 1 × 4 cm³ optical cell, was placed in a glass-walled water bath thermostated at 30 °C located in one arm of Michelson interferometer. The passage of each interference fringe is a measure of the degree of advancement of the reaction.

lation is to ensure that the physical conditions, such as temperature or concentration, are uniform throughout the sample. Gelation then occurs as a single, monotonic, transition. An example of such uniform gelation behavior in the system investigated in this paper [poly(acrylamide/bisacrylamide)] is found in our preliminary measurements of the time variation of the refractive index in the reacting solution. During gelation, the density of the solution, and hence the refractive index, increases. With an activated solution of acrylamide and bisacrylamide, suitably thermostated and placed in one arm of a Michelson interferometer, the reaction was followed by timing the passage of the interference fringes. It can be seen from the smooth curve of Figure 1 that the process is unique and monotonic.

The experiments described below do not fulfill the condition of homogeneity, in that a nonuniform constraint is applied to the samples. The presence of this nonuniformity permits the coexistence of gel and sol phases. After the gel point, the ensuing polymerization within the gel no longer exhibits the simple behavior of Figure 1 but instead adopts the unusual form of multiple gelations interpenetrating within the already existing gel structure.

Our original motivations for the two types of observation described here were (i) to investigate by centrifugation the effect of molecular size separation close to the gel point and (ii) to follow the construction of a correlation length and of possible larger scale heterogeneities after the gel point, by using SAXS. In neither case were we able to pursue these observations to the equilibrium condition, since the latter was under continuous modification from the imposed constraint. The two sets of observations, although different in detail, reveal a distinctive polymerization process that is common to both techniques.

Experimental Details

The gels were prepared in the form of precursor solutions of varying concentrations of acrylamide A and bisacrylamide B. To these solutions were added ammonium persulfate in aqueous solution to give an overall concentration of 0.7 g/L and, for the centrifugation experiments, tetraethylmethylenediamine (TEMED) at a volume fraction of 3 × 10^{-7}. No TEMED was necessary for the SAXS observations, since the intense X-ray beam from the synchrotron source generated sufficient free radicals in the solution to ensure polymerization within the beam cross section

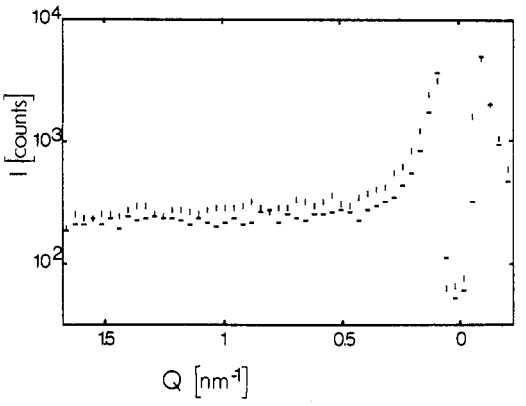

Figure 2. SAXS spectra from a polymerizing acrylamide/bisacrylamide solution (A = 0.05 g/mL, B = 0.003 g/mL), with an accumulation time of 100 s. Each point shown is the sum of five detector channels and is uncorrected for sample transmission. Horizontal bars, delay time 100 s (background spectrum); vertical bars, delay time 1500 s (principal gel point). The coordinate axis is linear, with the beam stop at position Q = 0.

in a reasonable time. The solutions were degassed to reduce the concentration of dissolved oxygen, before being introduced into the cells.

The sample holders used for SAXS consisted of thin mica windows separated by a 1-mm annular spacer of internal diameter 5 mm; this latter arrangement was connected by a slit in the spacer to a large outer reservoir in the stainless steel body, containing excess precursor fluid.

The X-ray scattering measurements were carried out on the D24 instrument at L.U.R.E., Orsay, using an incident wavelength of 0.16 nm, a sample–detector distance of 1.1 m, and a linear detector. Polymerization was carried out at room temperature (ca. 20 °C). The spectra were stored every 100 or 500 s, depending on the stage of the observations, and during the whole experimental run the X-ray beam was maintained uninterrupted. For the data analysis, the background used to calculate the corrected spectra was the first spectrum of the series from the same sample (t = 100 s), i.e., before polymerization had begun. This procedure ensures that sample and background have the same thickness. Figure 2 shows an example of a raw spectrum (t = 1500 s), together with the background spectrum.

The centrifuge (MSE Centriscan 75) Vinograd cells were 1.3 × 1.0 × 0.3 cm³. The ultracentrifuge measurements, carried out at the European Molecular Biology Laboratory at Grenoble, were performed at 20 °C, at moderate rotor speeds (≤20 000 rpm).

Observations

SAXS. The incident X-ray beam of rectangular cross section (3 × 0.6 mm) slightly ionizes the precursor fluid in its passage, thereby generating free radicals. Thus, within the beam, the gel polymerizes more rapidly than outside, and after a thousand or so seconds of exposure, a lens of polymerized gel of the same shape and size as the incident beam forms in the sample cell, adhering to the mica window. This change in appearance, caused by the increase in refractive index upon gelation, can be followed by simultaneously directing a low-power laser beam through the sample and detecting the transmission with a photodiode: the intensity fluctuations observed in the X-ray spectra are accompanied by corresponding fluctuations in the light throughput.

In Figure 3 are shown the observed scattered X-ray intensities for a single sample (A = 0.05 g/mL, B = 0.003 g/mL) at three different mean scattering vectors Q ($=4\pi\sin(\theta/2)/\lambda$, where θ is the scattering angle and λ the incident wavelength), as a function of time in the X-ray beam. The spectra were recorded every 100 s for 6000 s and, to improve the signal-to-noise ratio, at intervals of 500 s thereafter. While the intensity fluctuations at larger

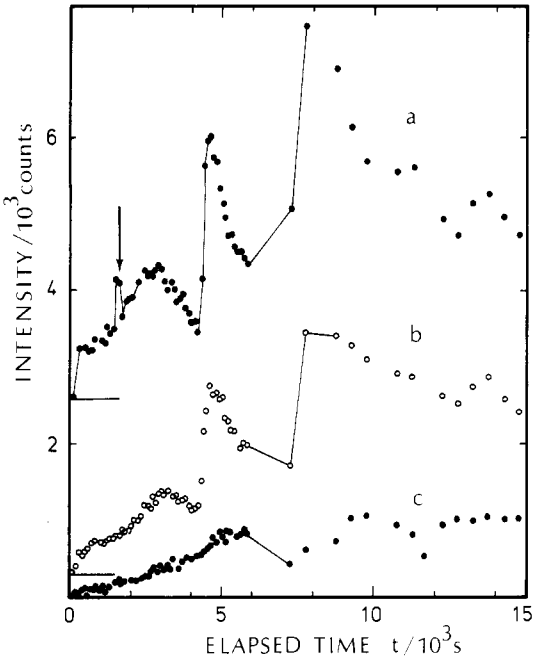

Figure 3. Variation of scattered X-ray intensity from an acrylamide/bisacrylamide solution (as in Figure 2) as a functon of time in the beam: (a) $Q = 0.19$ nm^{-1}; (b) $Q = 0.34$ nm^{-1}; (c) $Q = 1.23$ nm^{-1}. Each point is a sum over 20 detector channels with the mean Q indicated. The base lines of curves a and b are shown as short horizontal lines. The principal gel point is indicated by the arrow.

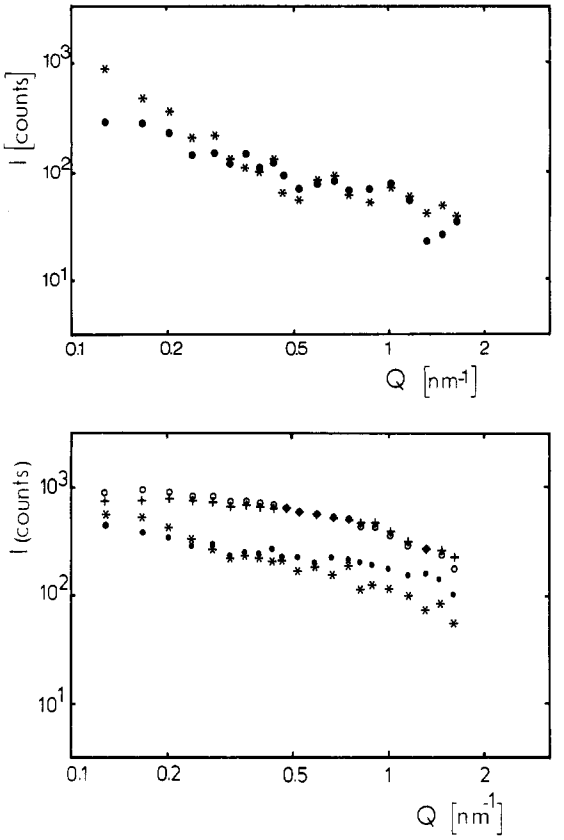

Figure 4. Corrected SAXS spectra, in a double-logarithmic representation, from a polymerizing acrylamide/bisacrylamide solution (as in Figure 2), at six different times: (a top) filled circles, 1300 s; stars, 1500 s (arrow in Figure 3), (b, bottom): stars, 2500 s; filled circles, 4100 s; open circles, 9750 s; crosses, 14250 s. The first four spectra are 100-s exposures, while the last two are 500 s (normalized to 100 s). The original 256-point spectra have been regrouped here: the 10 lowest Q points shown are each the sum of five detector channels, as in Figure 2. The six highest Q points are each the average of 20 channels (normalized to 5), and the intermediate points are the average of 10.

Q (1.23 nm^{-1}) appear to be of relatively small amplitude, those at the two smaller Q values become very large indeed.

During the first period of polymerization (≤4200 s), the shape of the scattering curves log I vs. log Q changes (Figure 4), while the total intensity increases. The curves can be approximately represented by two linear regions. In the Q range above about 0.5 nm^{-1}, the scattering function increases fairly smoothly with time, indicating an increasing density of closely spaced scatters: in the log/log representation of Figure 4, this part has a slope of nearly unity. At the lower scattering vectors (in the range 0.15 nm^{-1} ≤ Q ≤ 0.5 nm^{-1}), however, the slopes undergo large variations (Figure 5), starting at a value of roughly −1 and then passing through a sharply localized maximum of value −1.7 ± 0.2 at 1500 s. The initial slope subsequently falls to between −0.1 and −0.2, and the scattering curves tend to the Lorentzian shape characteristic of a gel or semidilute polymer solution. We associate this first sharp peak with the onset of the gel, identifying it with the conventional gel point (t_g = 1500 s).

The second and subsequent major intensity excursions in Figure 3 occur at intervals of approximately 3000 s. During these excursions, however, the initial slopes of the log I vs. log Q plots become steeper again, but their magnitude does not exceed unity.

It is worthwhile to add that such oscillations were observed in a large range of samples, although the amplitude of the intensity excursions decreased notably, but did not vanish, when the cross-linking concentration B was reduced to $B = 0$. In the case of $B = 0$, the X-ray beam generated a slight degree of permanent cross-linking, visualized as a small zone of higher refractive index at the center of the beam position.

When the coactivator TEMED is added to the precursor solution, the gelation process is greatly accelerated. In Figure 6 is shown the time dependence of the scattering intensities at three mean Q values (0.23, 0.38, and 1.24 nm^{-1}) from a precursor solution (A = 0.05 g/mL, B = 0.003

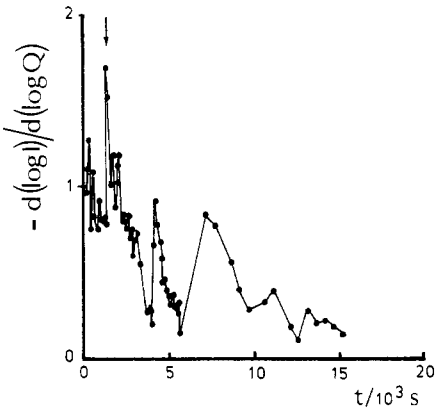

Figure 5. Variation in initial slope (between 0.15 and 0.5 nm^{-1}) of the SAXS spectra as a function of time in the beam. The principal gel point is indicated by an arrow.

g/mL) containing TEMED. Without an ionizing field, gelation would occur in about 1000–2000 s; in the X-ray beam, Figure 6 shows that the principal increase in scattering intensity (primary gelation) has already occurred within the first 100 s of exposure to the radiation. An attenuated secondary gelation appears at about 1500 s, after which no further evolution is observed. At the end of the run, the sample was found to have gelled throughout, albeit with a lens of more concentrated gel at the beam position. The high initial reaction speed has two conse-

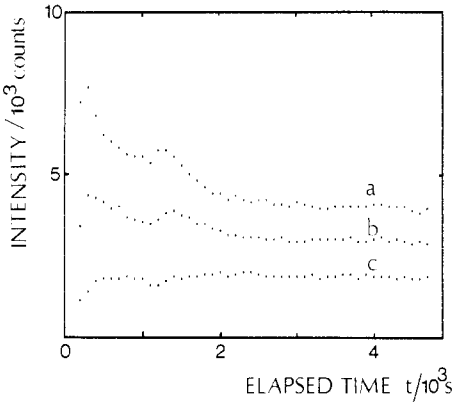

Figure 6. Variation in the scattered X-ray intensity from an acrylamide/bisacrylamide solution (A = 0.05 g/mL, B = 0.003 g/mL) containing TEMED at various mean scattering vectors: (a) Q = 0.23 nm^{-1}; (b) Q = 0.38 nm^{-1}; (c) Q = 1.24 nm^{-1}. As in Figure 3, each point is the sum of 20 original spectrum data points. TEMED was added at t = 0 and the sample placed in the X-ray beam at t = 120 s. Exposure time per spectrum, 100 s.

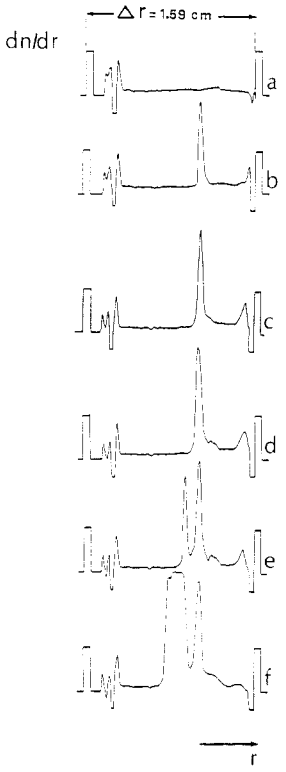

Figure 7. Schlieren recordings of the refractive index gradient dn/dr as a function of time during centrifugation (7000 rpm) in a gelating acrylamide/bisacrylamide solution (A = 0.08 g/mL, B = 0.002 g/mL). The features appearing in the first 4 mm (small r) of the spectra are artifacts caused respectively by the inner distance marker and bubbles at the top of both the sample and the reference cells: (a) t = 600 s; (b) t = 840 s; (c) t = 1080 s; (d) t = 1320 s; (e) t = 1560 s; (f) t = 3480 s. Between (e) and (f) two further polymerization avalanches, not shown here, occur.

quences. Because of limited scattering intensity, it is not possible to reduce further the frame exposure times without serious loss of information, and so the initial process cannot be followed in detail. The developed gel sample of the first frame (100 s) cannot be used as a background spectrum.

Centrifugation. The precursor fluid was mixed with TEMED to hasten polymerization and rotor speeds of about 7000 rpm were chosen to produce a modest acceleration field. The sample temeperature was stabilized at 20 °C.

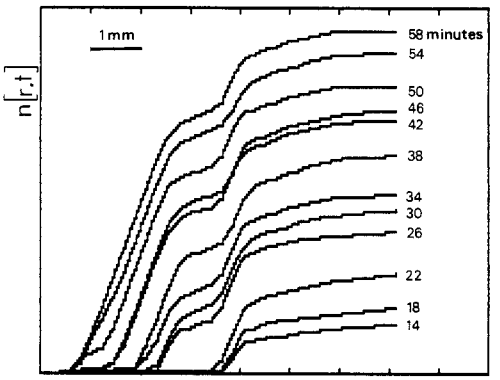

Figure 8. Integrated values of the refractive index $n(r,t)$ from 12 successive Schlieren scans at regular time spacings of 240 s in a gelating solution of acrylamide/bisacrylamide as in Figure 7. The numbers on the right refer to the time in minutes since the mixing of the precursor solution. The horizontal graduation scale is in units of 1 mm, and the vertical scale is arbitrary. The bottom of the cell is the right-hand edge of the figure. The region of deswollen gel just above this region is not included in the integration.

In Figure 7 is shown a series of separate optical scans, using the Schlieren detection system, of the polymerization of a polyacrylamide/water gel with A = 0.08 g/mL, B = 0.002 g/mL. A signal, proportional to the refractive index gradient dn/dr (where r is the radial distance in the cell) develops after roughly 15 min at a point in the cell that depends sensitively on the conditions of preparation and the delay between initiation and attaining the requisite rotor speed. The region to the right (large r) of the principal peak in Figure 7b is the gel, while that to the left is the unreacted sol. At later times (Figure 7e,f) new deposits of gel develop above the original interface, corresponding to fresh aggregation bursts in the sol phase.

It can be seen in Figure 7 that as the additional layers grow at the interface, no negative contribution to dn/dr forms deeper in the gel. This means that n is always a continuously increasing function of r, and therefore the polymerization avalanches that develop at the sol–gel interface are matched by a simultaneous increase in refractive index within the already formed gel below. This behavior is displayed in Figure 8, showing the integrated values of $n(r,t)$ in a sequence with regular time intervals between scans, in which the nonmonotonic rate of increase of n with time at fixed r inside the original gel phase is clearly visible. At the end of the experiment, inspection of the gels shows a layered structure, with steps of increasing refractive index (i.e., increasing concentration) at increasing depth in the cell.

Figure 9 shows further evidence that the secondary gelation events are not confined to the sol–gel interface, but occur inside the original gel. In this sequence of Schlieren curves the rotor speed was 20 000 rpm (A = 0.08 g/mL, B = 0.002 g/mL). Here, all of the secondary gelation up to 5000 s happens inside the original gel phase.

In the case of uncross-linked gels (solutions) similar discrete steps in refractive index occur as polymerization proceeds, but these disappear at longer times through diffusion of the polymer chains.

Discussion

In neither of the above experimental arrangements does the gel phase occupy the whole of the available sample space, the remaining volume being taken up by the sol, which therefore acts as a reservoir of fresh monomers for the gel. In the SAXS arrangement, gel does not form outside the beam area because too few free radicals are generated there; in the centrifuge cell, the acceleration field

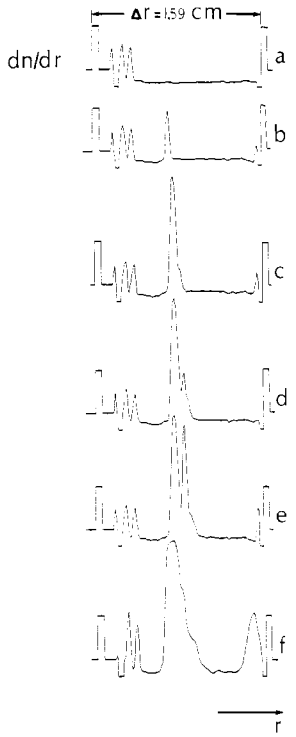

Figure 9. Schlieren recordings of the refractive index gradient dn/dr as a function of time during centrifugation (20 000 rpm) in a gelating acrylamide/bisacrylamide solution (A = 0.08 g/mL, B = 0.002 g/mL): (a) t = 540 s; (b) t = 780 s; (c) t = 1020 s; (d) t = 1500 s; (e) t = 1980 s; (f) t = 61200 s. The large feature visible at the right of recording (f), due to osmotic compression of the gel at the lower end of the cell, relaxes when the rotor speed is reduced.

sweeps away larger molecular aggregates as they form.

In both cases an estimate may be made of the characteristic time constants t_d necessary to transfer fresh monomers into the central gel region, assuming a translational diffusion coefficient D of approximately 10^{-5} cm^2/s. For the SAXS experiment the smallest dimension of the gel is initially about 0.6 mm, giving for the time constant

$$t_d = (0.03)^2/4D$$
$$= 20 \text{ s}$$

As polymerization proceeds, the region of gel encroaches beyond the direct beam into the surrounding area of sol, the thickness of the gel at the end of the experiment being about 2 mm. The corresponding diffusion time for monomers may thus be some 200 s. Diffusional access to the outer reservoir of the X-ray cells will take an order of magnitude longer in time (cf. Experimental Details).

For the centrifuge experiment, the characteristic distance between the top of the gel and the bottom is roughly 0.5 cm, giving a diffusion time constant of some 6000 s. These times may be compared with the intervals observed between successive gelation bursts, namely, ca. 3000 s for SAXS and ca. 1000 s in the case of centrifugation. It should be borne in mind that in the latter case, the estimated diffusional time constant t_d probably does not describe the true rate of mass transport, since the acceleration field may contribute significantly to the supply of fresh acrylamide into the gel.

It therefore appears that the transport time constants are comparable with the characteristic time between successive gelations and that the latter are fed by the incoming monomers and oligomers. Since no such sol reservoir exists under uniform conditions of gelation, it is clear why this phenomenon is not observed there. In the arrangement of Figure 6, the supply of fresh monomers is cut off when the sol reservoir itself becomes a gel; in this case, the delay was long enough for only one secondary gelation to take place.

The surprising feature of these results, however, remains the fact that the incoming monomers and oligomers do not appear to integrate continuously and smoothly into the existing gel structure. The results of the two experiments suggest rather that they contribute to independent gelations each with a corresponding induction time, forming interpenetrating networks of increasing total polymer concentration inside the original structure.

Such oscillatory gelation is possible only in the presence of nonlinear reaction rates, with, in addition, a delay in the supply of the reactants. Here, the delay in supply is provided by the diffusion of monomers through the existing gel. The requisite nonlinearity is found, first, in the induction time needed to exhaust inhibitors in the solution (residual oxygen, for example, is present in the sol reservoir) and, second, in the essentially nonlinear growth process of aggregation. The same conditions, namely, a large reservoir of monomers, delay due to diffusion, and a nonlinear aggregation process, are prerequisites in the closely analogous (spatially) oscillatory phenomenon of Liesegang rings.[8]

As to the time variation of the SAXS spectra, scattering measurements in the reaction bath are not usually recommended for observations of cluster sizes prior to gelation, on account of overlap between the intraparticle and interparticle structure factors.[9] Early on in the reaction, however, when the cluster sizes are small and far apart, the two structure factors are separate in Q space, and it may therefore be possible, given sufficient scattering intensity, to observe the true cluster size distribution for a brief period. We believe that the two spectra occurring close to 1500 s in Figures 3–5 correspond to this period, during which the initial slope of the spectra (-1.7 ± 0.2) corresponds to the value expected for percolation-like behavior.[5-7] Earlier in the reaction, however, the data of Figure 5 are in better agreement with the classical slope of -1.[5,10]

After the gel point, the scattering curves are not single Lorentzians, but the longest apparent correlation length obtained from them decreases slowly from roughly 5 nm at 2500 s to 2 nm before the abrupt increase beginning at 4300 s (Figures 3 and 5). Such behavior is to be expected in a gel of increasing concentration. However, the continuous modification of the gel due to the ionizing beam renders impossible any detailed comparison with equilibrium structures formed under uniform conditions.[11]

Conclusions

Our conclusions are as follows:

1. Polyacrylamide gels forming under the nonuniform conditions provided either by an intense X-ray beam or by a centrifuge display multiple-gelation behavior, each generation of gel interpenetrating with the structure of the previous gel generation. The new matter that feeds each generation is supplied as monomers or oligomers from the contiguous sol phase, and the gel concentration continues to increase until the supply of fresh radicals is exhausted. The reason for the discontinuous polymerization behavior seems to be related to the delay due to the diffusion of the monomers through the already established gel and to the nonlinear nature of the gelation. This behavior is a time analogue of the spatial fluctuations encountered in Liesegang rings.

2. The SAXS observations in the reaction bath indicate that in the earliest stages of the first-generation gel, the initial slopes of the log I vs. log Q are consistent with the

classical value of −1, but closer to the sol–gel transition a higher value is obtained (−1.7 ± 0.2), in agreement with the percolation theory and also with observations of other authors. The percolation-like behavior is of short duration (ca. $t_g/10$). Later in the reaction and in the subsequent gelations, such characteristic scattering features are probably masked by interference from neighboring clusters or from previous generations of gel.

Acknowledgment. We are grateful to the EMBL for access to and to B. Schoot for invaluable help with the Centriscan centrifuge. We also gratefully acknowledge instrumental time on the D24 instrument at L.U.R.E., Orsay, and the advice and comments of C. Williams, P. Vachette, and J. P. Benoit.

Registry No. (Acrylamide)(bisacrylamide) (copolymer), 25034-58-6.

References and Notes

(1) See, for example: Stauffer, D.; Coniglio, A.; Adam, M. *Adv. Polym. Sci.* **1982**, *44*, 103 and references therein.
(2) Gauthier-Manuel, B.; Guyon, E. *J. Phys. Lett. (Les. Ulis, Fr.)* **1980**, *41*, L-503.
(3) Adam, M.; Delsanti, M.; Durand, D. *Macromolecules* **1985**, *18*, 2285.
(4) Allain, C.; Amiel, C. *Phys. Rev. Lett.* **1986**, *56*, 1501.
(5) Schosseler, F.; Leibler, L. *J. Phys. Lett. (Les Ulis, Fr.)* **1984**, *45*, L-501.
(6) Candau, S. J.; Ankrim, M.; Munch, J. P. In *Physical Optics of Dynamic Phenomena and Processes in Macromolecular Systems*; Sedlacek, B., Ed.; W. de Gruyter: Berlin, 1985; p 145.
(7) Bouchaud, E.; Delsanti, M.; Adam, M.; Daoud, M.; Durand, D. *J. Phys. (Les. Ulis, Fr.)* **1986**, *47*, 1273.
(8) Feeney, P. J.; Gilbert, R. G.; Napper, D. H. *J. Colloid Interface Sci.* **1985**, *107*, 159.
(9) de Gennes, P.-G. *Scaling Concepts in Polymer Physics*; Cornell: Ithaca, NY, 1979.
(10) Stockmayer, W. H. *J. Chem. Phys.* **1944**, *12*, 125.
(11) Hecht, A.-M.; Duplessix, R.; Geissler, E. *Macromolecules* **1985**, *18*, 2167.

Interaction of Anionic Surfactants with Gelatin: Viscosity Effects

J. Greener,*† B. A. Contestable,† and M. D. Bale‡

Research Laboratories—Diversified Technologies Group, and Research Laboratories—Life Sciences Division, Eastman Kodak Company, Rochester, New York 14650.
Received December 3, 1986; Revised Manuscript Received May 18, 1987

ABSTRACT: Interactions of anionic surfactants with an alkali-processed gelatin above its isoelectric point were studied over a wide range of conditions. Extraordinarily large increases in viscosity were observed for some systems above a critical surfactant concentration, which nearly coincided with the critical micelle concentration for the corresponding gelatin–surfactant mixture. The general thickening effect is characterized by four distinct regimes corresponding to the level of surfactant in the gelatin solution. The extent of thickening was closely related to surfactant type, surfactant/gelatin composition, and ionic strength, with lesser effects exerted by gelatin type and pH level. The specific architecture of the surfactant molecule, particularly the size of the aliphatic moiety, had a decisive effect on the critical concentration for the onset of thickening and the ultimate thickening extent. A simple model, based on a cooperative micellar binding mechanism, is proposed to explain some of these observations.

Introduction

Interactions between surfactant molecules and synthetic or natural polymers have been studied extensively over the past several decades. These interactions have received considerable attention because of their ability to impart significant changes to the interfacial, rheological, and physicochemical properties of polymer systems, with important implications in various pharmaceutical, biomedical, food processing, and photographic applications.[1] Surfactant–polymer interactions involve various modes of association facilitated by dipole–dipole, ion–dipole or ion–ion forces. Nagarajan and Kalpakci[2] discuss six possible types of associations involving either individual surfactant molecules or surfactant clusters (micelles). In studies on mixtures of nonionic polymers with anionic surfactants,[1-3] a systematic drop in the critical micelle concentration (cmc) and moderate increases in viscosity have been observed. Evidence from nuclear magnetic resonance (NMR)[4] and neutron scattering[5] studies suggests the existence of polymer–micelle complexes in such systems. When both the surfactant and the polymer are charged, the interactions are dominated by strong Coulombic forces. Generally, the interaction of a surfactant with an oppositely charged polyelectrolyte results in precipitation.[6,7] Solubility of the polymer is, however, still possible at low concentrations of surfactant where complexation is not extensive and at very high concentrations where the complex is solubilized by excess surfactant. Large changes in viscosity at both concentration regimes have been observed.[8] Because of the unique electrolytic character of proteins, phenomena involving protein–surfactant interactions are especially intriguing. The ability of surfactants to denature and precipitate globular proteins and the disinfecting action of cationic detergents on bacteria are well-known.[9,10] Because of the diversity of polypeptide structures, it is not possible to generalize the consequences of interactions of proteins with surfactants. However, for denatured proteins one can distinguish two general cases:[10] (a) mixtures of anionic surfactants with proteins above the isoelectric point (IEP) (below the IEP for cationic surfactants) and (b) mixtures of anionic surfactants with proteins below the IEP (above the IEP for cationic surfactants). Since the protein has a net positive charge below the IEP and can be considered a "cationic" polymer, the interactions with anionic surfactants are dominated by precipitation phenomena. Above the IEP, the interactions lead to formation of stable, fully solubilized complexes which can lead to drastic changes in the topology and conformation of the protein molecule in solution.

In this study, we set out to explore the interaction of gelatin, a well-characterized denatured protein, with anionic surfactants, covering a wide range of compositions and conditions. As our main tool we used viscometry, which is convenient and particularly effective in probing

† Diversified Technologies Group.
‡ Life Sciences Division.

0024-9297/87/2220-2490$01.50/0